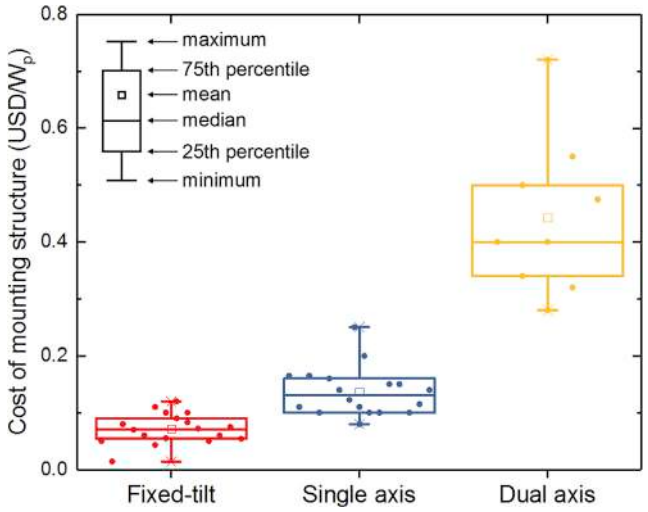

Figure 7. Surveyed Cost of Mounting Structure for Fixed-Tilt, Single-Axis, and Dual-Axis Tracker PV Installations

systems (a linear cost relation is assumed). For PV insurance (c_{insu}), 0.3% of the initial investment is required to be paid every year.[30] With the presented values, the lifetime system cost can be calculated for any PV installation design and module technology. Thereafter, LCOE can be obtained.

RESULTS

Global Yield Comparison for HSAT and TSAT

Depending on the location, preference to use HSAT or TSAT may vary. Figure 8 presents the percentage difference in yield between these mounting structures for monofacial (1) and bifacial (2) modules. We find that TSAT installations are preferred for higher latitude locations and generate up to 19% more energy, with the exception of a small belt around the equator. In this belt, HSAT configurations generate up to 6.7% and 4.4% more yield for monofacial and bifacial installations, respectively. In subsequent sections, energy yield results for single-axis tracker installations refer to that of the configuration (HSAT or TSAT) that gives higher energy yield in each particular location (Figure 8).

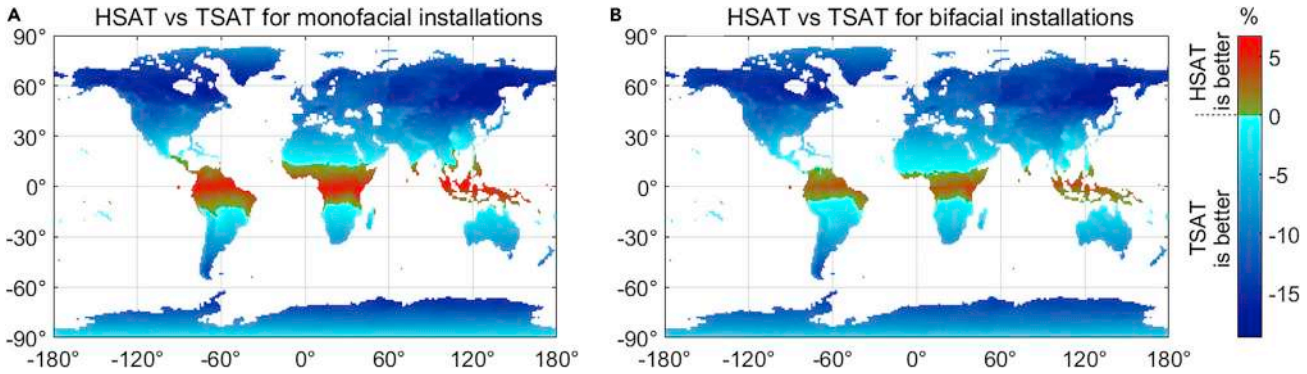

Figure 8. Performance Comparison between Single-Axis Trackers

Relative difference in energy yield between HSAT and TSAT installations for (A) monofacial systems and (B) bifacial systems. Positive values (green and red colors) mark locations in which HSAT installations generate higher yield than their TSAT counterparts where the opposite result (negative values) are marked with blue.

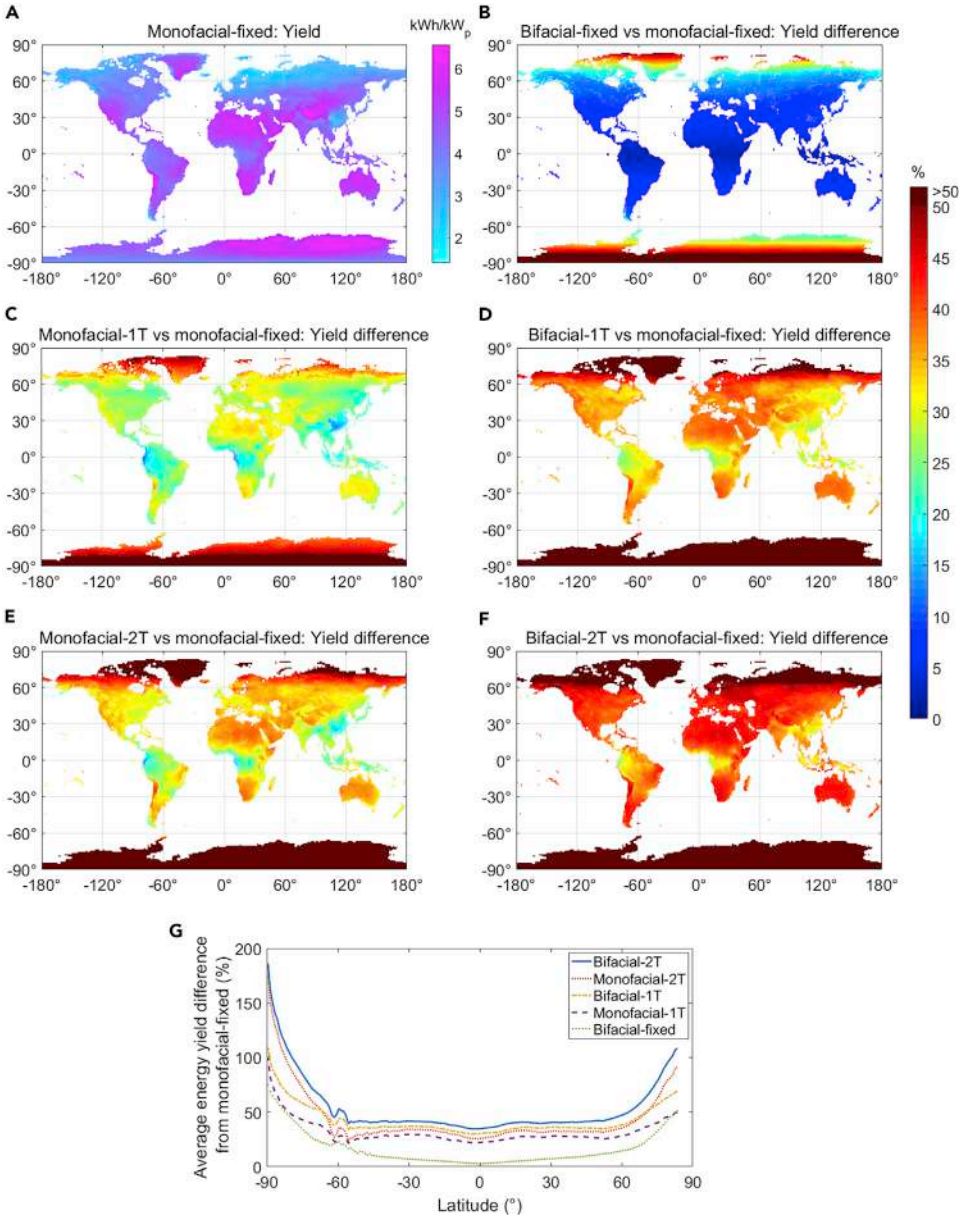

Figure 9. Worldwide Energy Yield Results

(A) Daily average energy yield for the monofacial fixed-tilt installation. The following plots present the percentage difference between the energy yield (with respect to monofacial fixed-tilt) for (B) bifacial-fixed, (C) monofacial-1T, (D) bifacial-1T, (E) monofacial-2T, and (F) bifacial-2T. In (G), the average energy yield difference for the different systems with respect to the monofacial fixed-tilt reference is shown (the presented values are the average from all the analyzed longitude locations at a particular latitude).

Energy Yield Analysis

Figure 9A shows the daily average energy yield in kWh/kWp worldwide for monofacial fixed-tilt installations. The following plots (Figures 9B–9F) show the yield difference of the other installation designs (y_{other}) compared with the monofacial fixed-tilt reference ($y_{mono,fix}$):

$$\Delta y = y_{other} \Big/ y_{mono,fix} - 1 \qquad \text{(Equation 4)}$$

Please cite this article in press as: Rodríguez-Gallegos et al., Global Techno-Economic Performance of Bifacial and Tracking Photovoltaic Systems, Joule (2020), https://doi.org/10.1016/j.joule.2020.05.005

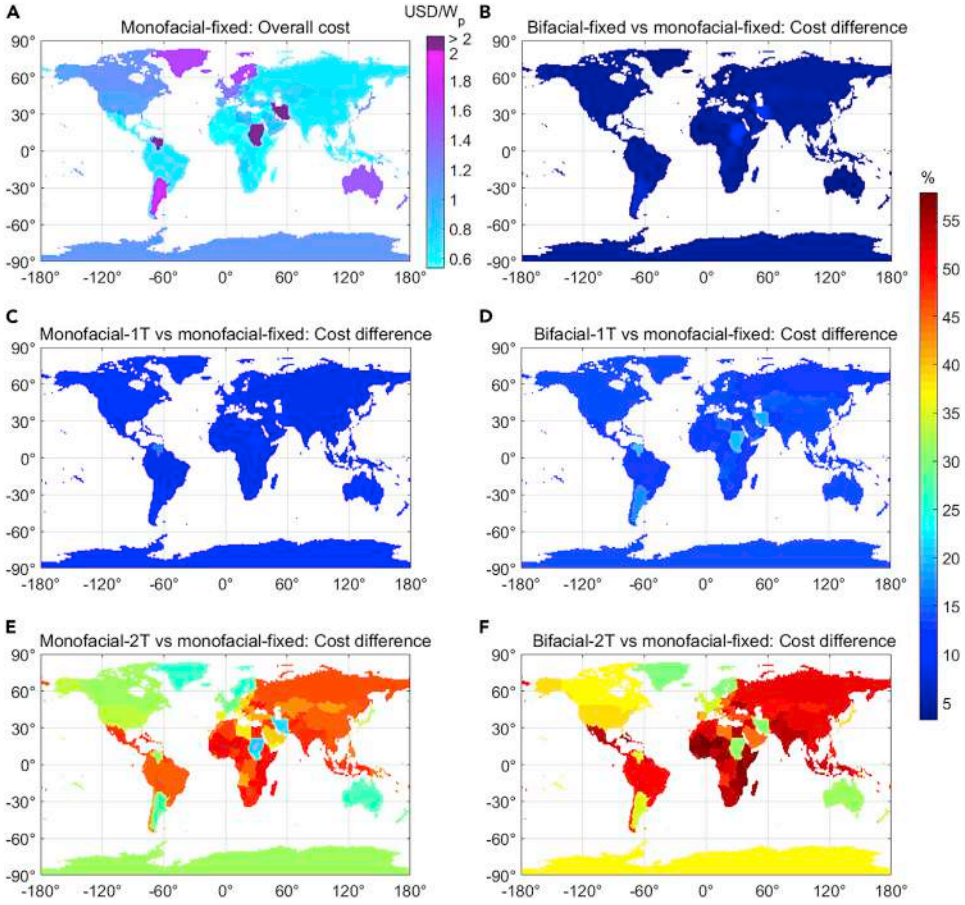

Figure 10. Worldwide Cost Results

(A) Overall specific system cost in USD/W_P during its lifetime for the monofacial-fixed-tilt installation.

(B–F) The following plots present the percentage difference between the overall system cost (with respect to monofacial fixed-tilt) for (B) bifacial-fixed, (C) monofacial-1T, (D) bifacial-1T, (E) monofacial-2T, and (F) bifacial-2T.

Figure 9G shows the average yield improvement per latitude for each configuration. All combinations of tracking and bifacial systems improve yield, with improvements of more than 50% possible in very high latitudes. In general, with the same mounting structure, bifacial configuration outperforms monofacial configuration. Tracker configurations outperform fixed-tilt configurations significantly, with dual-axis tracker installations having marginally higher yield than one axis. However, bifacial-1T has a slightly better performance than monofacial-2T within a latitude range of $\pm 60^{\circ}$, highlighting the advantage of using bifacial tracking in these regions. On the other hand, monofacial-1T clearly has a large gain from bifacial fixed-tilt installations.

Overall System Cost

Figure 10A displays the calculated overall PV system cost (C_{PV}) during its lifetime for a monofacial fixed-tilt installation in USD/Wp, while the other plots show the percentage difference on the overall cost of the other installation designs (c_{other}) compared with the monofacial fixed-tilt reference ($c_{mono,fix}$):

$$\Delta c = c_{other} \,/\, c_{mono,fix} - 1 \qquad \text{(Equation 5)}$$

Please cite this article in press as: Rodríguez-Gallegos et al., Global Techno-Economic Performance of Bifacial and Tracking Photovoltaic Systems, Joule (2020), https://doi.org/10.1016/j.joule.2020.05.005

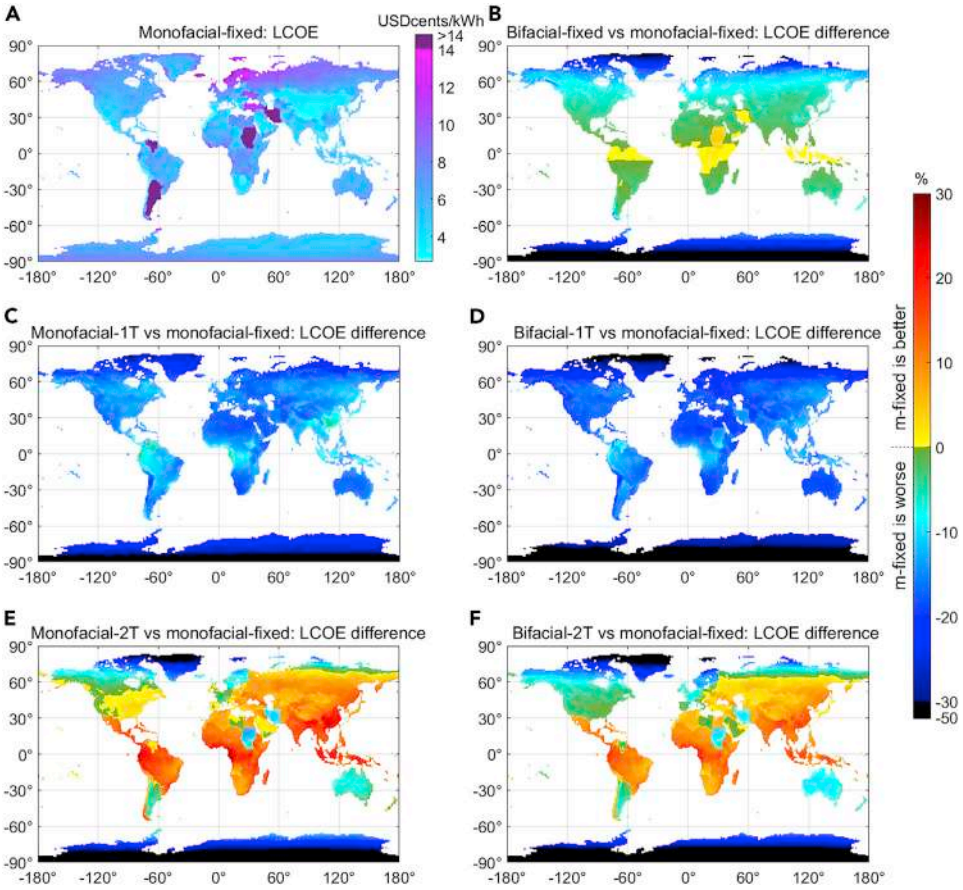

Figure 11. Worldwide LCOE Results

(A) Estimated LCOE worldwide for monofacial fixed-tilt (m-fixed) installations.

(B–F) The following plots present the percentage difference between the LCOE (with respect to monofacial fixed-tilt) for (B) bifacial-fixed, (C) monofacial-1T, (D) bifacial-1T, (E) monofacial-2T, and (F) bifacial-2T.

Figure 10B shows that the overall cost of bifacial-fixed systems is slightly higher than the one from its monofacial counterpart because of the higher inverter, installation, and O&M cost, as discussed in Global Techno-Economic Performance Calculation. All tracker installations feature higher costs than the conventional fixed-tilt installation due to higher installation and O&M costs (also discussed in Global Techno-Economic Performance Calculation). Yet, while one-axis tracker installations typically incur less than 10% higher system costs, two-axis tracker installations are between 30% and 60% more expensive than conventional monofacial fixed-tilt installations. These considerably higher system costs for two-axis tracker systems are mainly due to the high cost of their mounting structure (see Figure 7).

LCOE Analysis

LCOE results are presented in Figure 11. Similar to Figures 9 and 10, we first plot the calculated LCOE baseline for monofacial fixed-tilt installations in (A), and then in (B) to (F) we plot the relative LCOE differences for the other systems ($LCOE_{other}$) compared with the monofacial fixed-tilt reference ($LCOE_{mono,fix}$):

$$\Delta LCOE = LCOE_{other} \,/\, LCOE_{mono,fix} - 1 \qquad \text{(Equation 6)}$$

We find that bifacial installations with single-axis trackers reach the lowest LCOE almost everywhere (i.e., 93.1% of the total land area), while their monofacial

Please cite this article in press as: Rodríguez-Gallegos et al., Global Techno-Economic Performance of Bifacial and Tracking Photovoltaic Systems, Joule (2020), https://doi.org/10.1016/j.joule.2020.05.005

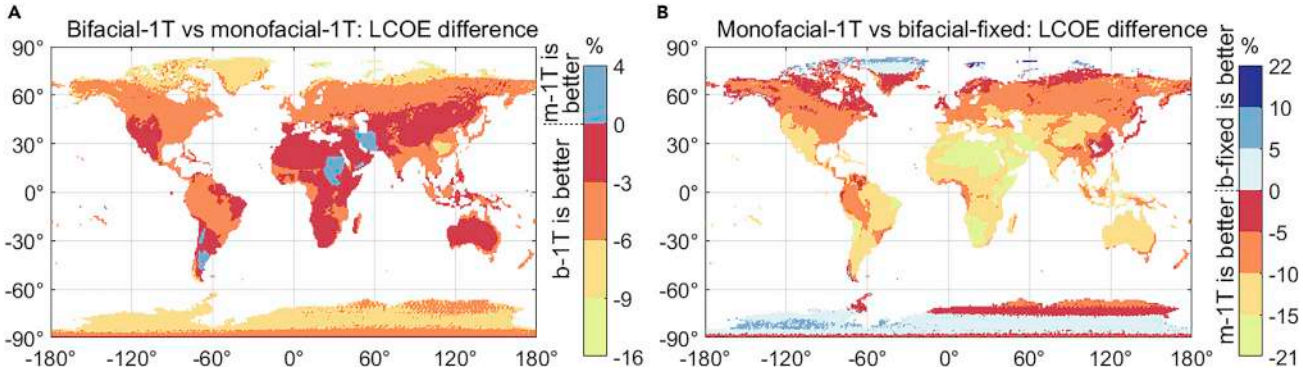

Figure 12. LCOE Technology Comparison

LCOE difference between (A) bifacial-1T (b-1T) with respect to monofacial-1T (m-1T) installations, and (B) monofacial-1T with respect to bifacial-fixed (b-fixed) installations.

counterparts achieve the lowest LCOE in only 3.1% of the land area. In addition, bifacial two-axis tracker installations reach the lowest LCOE only for remote areas very close to the poles, at latitudes beyond 70°, accounting for 3.8% of the total land area. Furthermore, monofacial single-axis trackers achieve the second lowest LCOE values for 87.9% of the land area.

On the one hand, these findings are explained by the fact that one-axis tracker systems generate comparably high yields (Figure 9), while requiring only marginally higher cost (Figure 10) compared with fixed-tilt installations. On the other hand, although two-axis tracker systems in general generate the highest yield, their considerably more expensive mounting structure (see Figures 7 and 10) outweighs the benefits in energy generation.

In addition, Figure 11 also reveals that, compared with conventional fixed-tilt installations, bifacial fixed-tilt installations feature higher LCOE values close to the equator (compare Figures 11A and 11B), whereas tracker installations with bifacial modules reach, in general, lower LCOE values compared with their monofacial counterparts (compare Figures 11C–11F).

To highlight the performance improvement of bifacial one-axis trackers with respect to their monofacial counterparts, the percentage difference on LCOE between these technologies are shown in Figure 12A (positive values are for the cases when bifacial-1T systems have a higher LCOE than monofacial-1T). This figure shows that for most locations of interest, the LCOE from bifacial-1T systems are typically 0%–6% lower than the ones from their monofacial counterparts. The comparative advantage from bifacial-1T systems tends to increase when moving closer to the poles.

Figure 12B shows the percentage difference in LCOE between monofacial-1T and bifacial fixed-tilt systems (positive values are for the cases when monofacial-1T systems have a higher LCOE than bifacial fixed-tilt). In general, the tracking properties from monofacial-1T systems result in a considerable LCOE reduction compared with bifacial fixed-tilt systems (reaching values up to 21%). However, only for locations close to the poles, the properties of bifacial modules to capture light from both sides becomes more influential and results in lower LCOE values.

Table 3. Details on the Selected Countries to Perform the LCOE Sensitivity Analysis

	Country's Accumulated Installed PV capacity till 2018 (GW_p)[3]	Latitude (°)	Longitude (°)	Mean Daily GHI (W/m^2)[32]
China (Zhongba)	176.1	30.5	83.5	260
USA (Yuma)	62.2	32.5	−114.5	238
Japan (Mine)	56.0	35.5	138.5	167
Germany (Dornstetten)	45.4	48.5	8.5	145
India (Kavalanahalli)	32.9	14.5	76.5	239
Italy (San Biagio Platani)	20.1	37.5	13.5	198
UK (Liskeard)	13.0	50.5	−4.5	135
Australia (St. George Ranges)	11.3	−19.5	124.5	272
France (Meyreuil)	9.0	43.5	5.5	188
South Korea (Uiseong County)	7.9	36.5	128.5	176

Sensitivity Analyses

While the previous results aimed to provide a comprehensive comparison among the different configurations worldwide, the assumed weather parameters, module properties, and cost figures may be different for different projects. Therefore, in an effort to examine the uncertainty on LCOE due to assumed parameter values, sensitivity analyses are carried out for the ten countries with the highest accumulated installed PV capacity till 2018,[3] choosing locations with high GHI values. The countries' parameters are provided in Table 3.

Monte Carlo

We used Monte Carlo simulation for the sensitivity analysis applying the approach presented in Chang et al.[69] Here, the input parameters (weather, module, and cost parameters) are assumed to have a two-half-log-normal distribution with median (μ), 10th percentile (Y_{Low}), and 90th percentile (Y_{High}). As indicated in Chang et al.,[69] Y_{Low} and Y_{High} can be considered to be the ones limiting the range after which it would be surprising to find values beyond it. The median values of the input parameters are set to the ones defined in Global Techno-Economic Performance Calculation as these were used in the previous sections. The Y_{Low}/Y_{High} values are defined in Table 4 with its respective reference. For the other parameters, no trustworthy data were obtained to estimate their Y_{Low} and Y_{High} values, therefore, these are assumed to be 0.95 and 1.05 of μ, respectively.

In this analysis, a total of 10,000 random samples were used per variable, and their respective LCOE were estimated for all system designs. Results are shown in Figure 13 with box-plots and distribution functions.

Mean LCOEs and standard deviations (SD) from Figure 13 are summarized in Table 5. Considering the results summarized there, we find that the picture about which system performs best becomes more nuanced.

As found previously, the bifacial-1T design features, in general, the lowest LCOE in all locations. Yet, monofacial-1T systems achieve LCOEs that are very similar, and fall within the calculated SDs of bifacial-1T systems. This result is not necessarily an

Please cite this article in press as: Rodríguez-Gallegos et al., Global Techno-Economic Performance of Bifacial and Tracking Photovoltaic Systems, Joule (2020), https://doi.org/10.1016/j.joule.2020.05.005

Table 4. Y_{Low} and Y_{High} Values for Different Parameters of Interest

	Y_{Low}	Y_{High}
Weather-Related Parameters		
GHI, DNI and DHI[70]	0.95 of reference year	1.05 of reference year
I_f (I_r) Note: Y_{Low} and Y_{High} Estimation from Data Provided In Validation of Irradiance Calculation Methodology	0.98 (0.89) of value obtained from modeling	1.06 (1.25) of value obtained from modeling
Cost of Mounted Structure (from Figure 7)		
Fixed-Tilt [USD/W_p]	0.013	0.15
1T [USD/W_p]	0.08	0.25
2T [USD/W_p]	0.28	0.72
Module-Related Parameters for Monofacial (Bifacial) Technologies		
Cost [USDcents/W_p][71] Note: Monofacial/Bifacial Modules Are Assigned the Same Cost for Simplicity	24 (24)	42 (42)
Module Front Power under STC [Wp]	250 (265)	365 (330)
b [%]	−(75)	−(93)
γ [%/°C]	−0.493 (−0.47)	−0.3 (−0.28)
β_0 [%]	2 (0.7)	3 (3)
β_1 [%/Year]	0.45 (0.25)	0.73 (0.59)
INOCT [°C]	38 (38)	47 (46)

The values of the module performance parameters were obtained by comparing multiple datasheets from different monocrystalline Si module manufacturers.

indication that the LCOEs of both systems are indistinguishable, as many of the considered parameters would vary similarly for either architecture, but it shows that advantages based on fixed values should be taken in context. We have marked in Table 5 all architectures that fall within the minimum range, given calculated SDs. Considering the distribution of values, finding the system that generates the lowest LCOE is, in reality, probably more complex than what is shown in Figures 11 and 12. Exact local conditions need to be taken into account to generate a comprehensive comparison in each case. Our analysis can help as a starting point by providing a guideline of which system performs best under ideal conditions, and how much of an economic advantage can be expected.

Looking at 2T systems, a large spread in calculated LCOE values is observed, which is mainly due to the large range of values related to the 2T mounting structure costs (as seen in Figure 7). Results in Figure 13 and Table 5 indicate that, if 2T mounting structures fall on the lower end within the considered range, or become even cheaper, 2T tracking systems could become a competitive option.

Region Sensitivity

For this analysis, the values from two key cost parameters, i.e., module and mounting structure costs, have been modified within a large range of 1%–1,000% (where 100% corresponds to the original values provided in Global Techno-Economic Performance Calculation) to account for a wide range of cost scenarios. The technology which achieves the lowest LCOE for the locations defined in Table 3 are color coded and the resulting "phase diagrams" are presented in Figure 14. Note that the plots are scaled logarithmically.

Please cite this article in press as: Rodríguez-Gallegos et al., Global Techno-Economic Performance of Bifacial and Tracking Photovoltaic Systems, Joule (2020), https://doi.org/10.1016/j.joule.2020.05.005

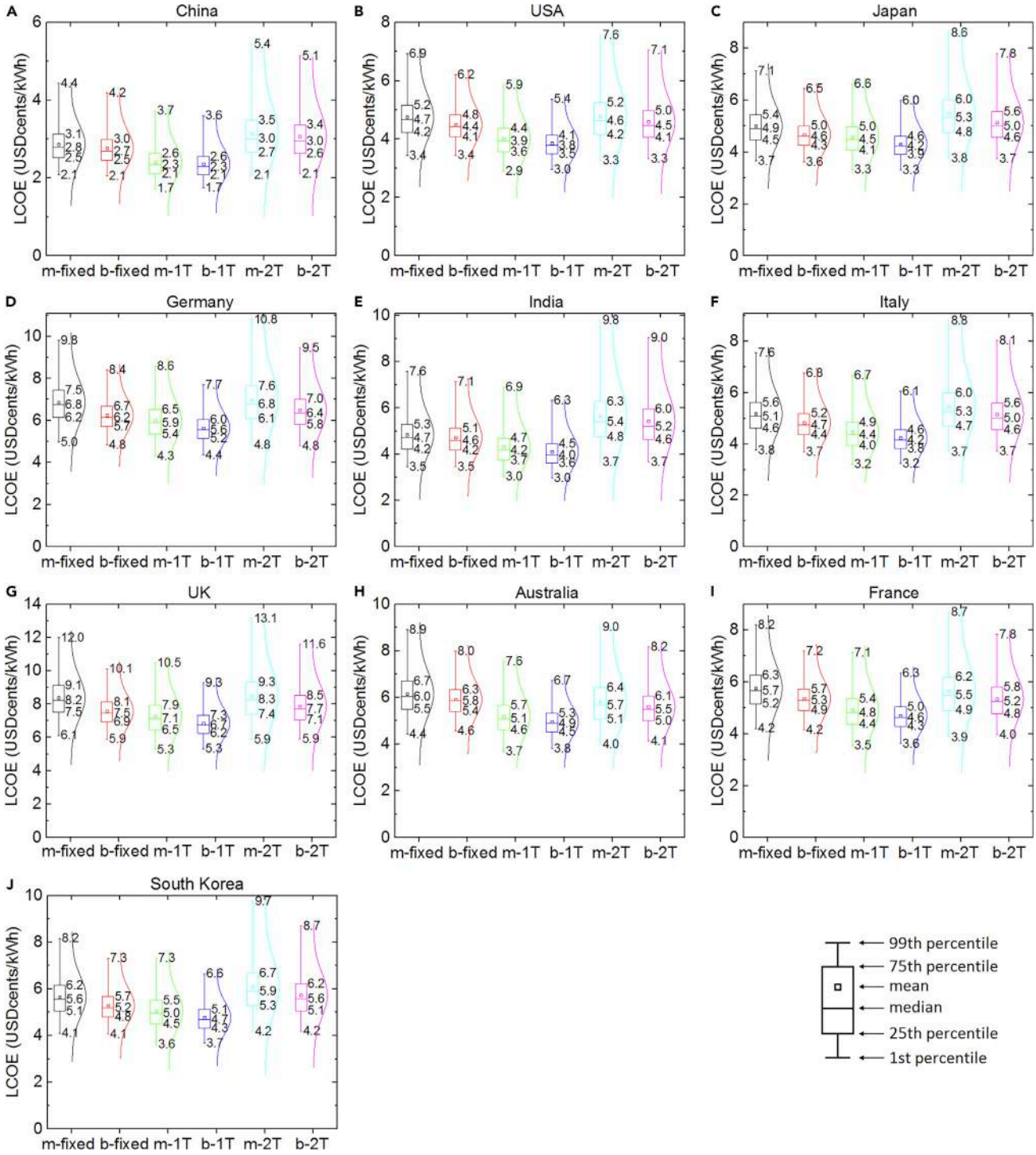

Figure 13. Monte Carlo Results on LCOE Designs Based on the Selected Mounting Structures for Monofacial and Bifacial Module Installations

The values of the 99th, 75th, 25th, and 1st percentile, as well as the median, are also provided. m, monofacial; b, bifacial.

The results show that the lowest cost for bifacial one-axis tracking systems are robust over a wide range of parameter changes. Mounting structure cost as well as module cost would have to fall by at least 50% for another configuration, monofacial one-axis trackers, to become the most economic one in the most competitive region—China.

Please cite this article in press as: Rodríguez-Gallegos et al., Global Techno-Economic Performance of Bifacial and Tracking Photovoltaic Systems, Joule (2020), https://doi.org/10.1016/j.joule.2020.05.005

Table 5. LCOE Mean (SD) Values Obtained from the Analyzed Locations from Figure 13

	Monofacial-Fixed	Bifacial-Fixed	Monofacial-1T	Bifacial-1T	Monofacial-2T	Bifacial-2T
China (Zhongba)	2.9 ± (0.5)	2.8 ± (0.4)[a]	2.4 ± (0.4)[b]	2.4 ± (0.4)[b]	3.1 ± (0.7)	3.1 ± (0.6)
USA (Yuma)	4.8 ± (0.7)	4.5 ± (0.6)	4.0 ± (0.6)[a]	3.9 ± (0.5)[b]	4.8 ± (0.9)	4.6 ± (0.8)
Japan (Mine)	5.0 ± (0.7)	4.7 ± (0.6)[a]	4.6 ± (0.7)[a]	4.3 ± (0.6)[b]	5.5 ± (1.0)	5.1 ± (0.8)
Germany (Dornstetten)	6.9 ± (1.0)	6.2 ± (0.8)[a]	6.0 ± (0.9)[a]	5.6 ± (0.7)[b]	7.0 ± (1.3)	6.5 ± (1.0)
India (Kavalanahalli)	4.8 ± (0.9)	4.7 ± (0.8)[a]	4.3 ± (0.8)[a]	4.1 ± (0.7)[b]	5.6 ± (1.3)	5.4 ± (1.1)
Italy (San Biagio Platani)	5.2 ± (0.8)	4.8 ± (0.7)[a]	4.5 ± (0.7)[a]	4.2 ± (0.6)[b]	5.5 ± (1.1)	5.2 ± (0.9)
UK (Liskeard)	8.4 ± (1.2)	7.6 ± (0.9)a	7.3 ± (1.1)[a]	6.8 ± (0.8)[b]	8.5 ± (1.5)	7.9 ± (1.2)
Australia (St. George Ranges)	6.2 ± (0.9)	5.9 ± (0.7)	5.2 ± (0.8)[a]	5.0 ± (0.6)[b]	5.8 ± (1.0)	5.6 ± (0.8)[a]
France (Meyreuil)	5.8 ± (0.9)	5.4 ± (0.6)	4.9 ± (0.8)[a]	4.7 ± (0.6)[b]	5.6 ± (1.0)	5.4 ± (0.8)
South Korea (Uiseong County)	5.7 ± (0.9)	5.3 ± (0.7)[a]	5.1 ± (0.8)[a]	4.8 ± (0.6)[b]	6.1 ± (1.2)	5.7 ± (1.0)

The cells with the lowest mean value are with bold font while underline is applied to the ones with mean values which fall under the uncertainty of the bold font cells.

[a]Cells with mean values that fall under the uncertainty of the cells with the lowest mean value.

[b]Cells with the lowest mean value.

In all other regions, costs would need to fall by about one order of magnitude before another configuration; in most cases bifacial two-axis trackers generate the lowest LCOE. These results further emphasize the potential of bifacial one-axis tracking systems to transform the PV market.

DISCUSSION

Based on the findings of this paper, we make the following observations:

(1) The optimum type of one-axis tracking system can be chosen as a function of geographical location. For locations very close to the equator, the use of HSAT systems is recommended as they can produce up to 6.7% more energy for monofacial and 4.4% for bifacial modules than TSAT systems. Meanwhile, for locations with latitudes above 15° (for monofacial systems) and 10° (for bifacial systems), our results indicate TSAT systems have energy advantage that increases with latitude and can reach up to 19%.

(2) With respect to energy yield, Table 6 shows the average ratio in energy generation of one particular technology (column) divided by the competing architectures (row) at latitudes within a range of ±60°. This table indicates that going from monofacial to bifacial adds, for the adopted specifications and models, on average 7% to yield, going from fixed-tilt to 1T adds 26% and going from fixed-tilt to 2T adds 31%. Furthermore, going from 1T to 2T adds 4% to average yield. The table also shows that yield gains from bifacial and tracking tend to be additive, i.e., using bifacial modules improves yield by its relative advantage (7% here) on top of yield gains through tracking (in our analysis, 7% on top of 26% results in a total gain of 35%).

(3) The LCOE for bifacial single-axis tracker installations is the lowest for the majority of the world (93.1% of the analyzed land area), while the monofacial single-axis tracker systems achieve the second lowest LCOE in 87.9% of the analyzed land area. This highlights the advantage of 1T designs as they are able to generate higher energy production than fixed-tilt systems without such a high cost as required for 2T systems. Hence, under the current market situation, 1T systems are cost effective and preferable. The average LCOE ratio of the different considered PV system architectures (column) divided by all other systems (row) at latitudes within a range of ±60° is presented in Table 7.

Please cite this article in press as: Rodríguez-Gallegos et al., Global Techno-Economic Performance of Bifacial and Tracking Photovoltaic Systems, Joule (2020), https://doi.org/10.1016/j.joule.2020.05.005

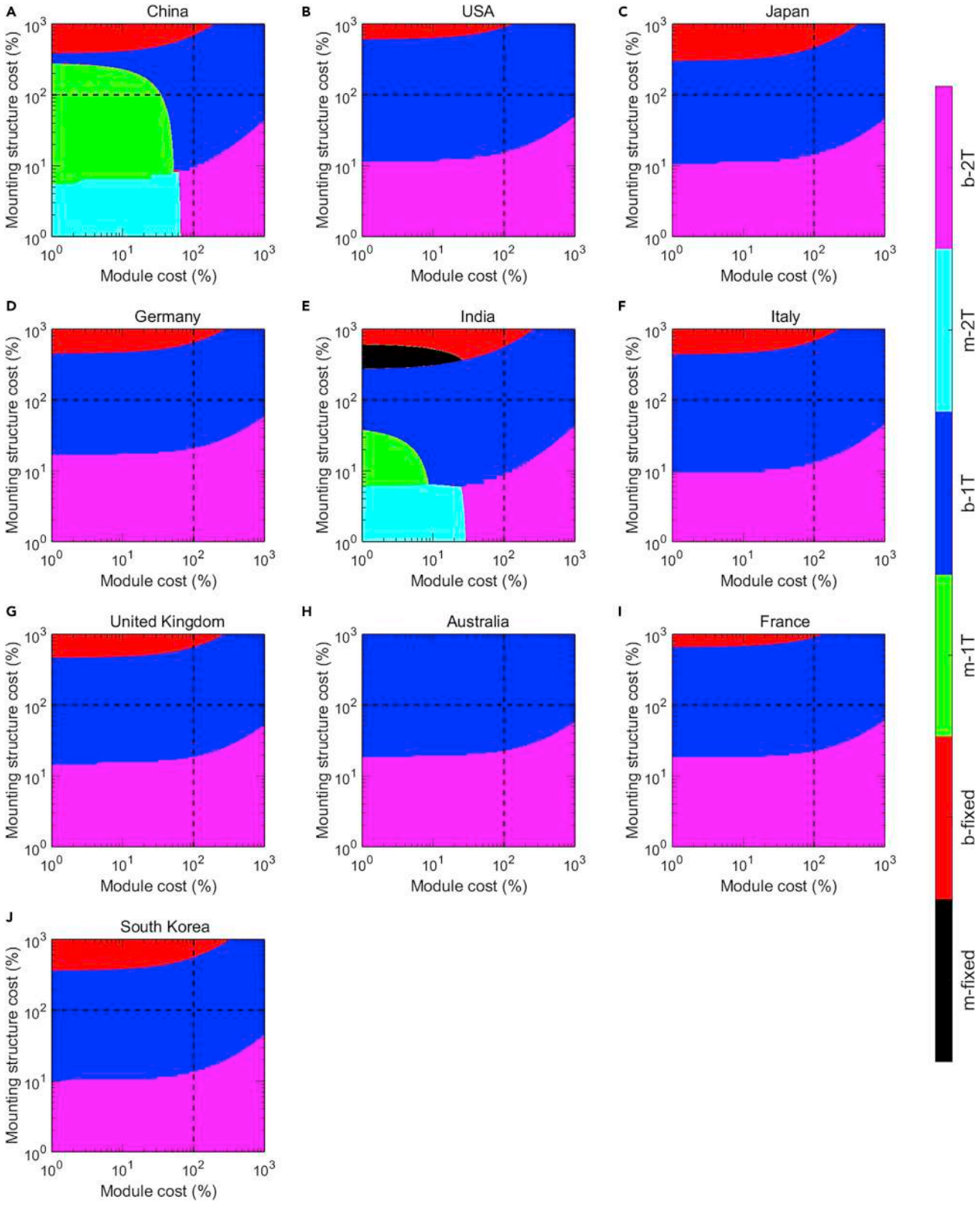

Figure 14. Sensitivity Analysis Based on Variations on the Module Cost, i.e., Monofacial and Bifacial Modules, versus Variations on the Mounting Structure Cost, i.e., Fixed-Tilt, 1T, and 2T

The designs with the lowest LCOE is presented. Module and mounting structure costs set to 100% corresponds to the original values provided in Global Techno-Economic Performance Calculation. m, monofacial; b, bifacial

This table shows a reduction on LCOE (3%) when using bifacial systems with respect to their monofacial counterparts. With respect to trackers, 1T systems achieve an average reduction on LCOE of ~14% compared with fixed-tilt systems while 2T systems increase the LCOE by 8%.

(4) Although the energy generation from dual-axis trackers is the highest, they produce, in general, the highest LCOE values (except for locations close to the poles). Currently, the main limitation for these systems is the considerably high cost of their mounting structure, as shown in Figure 7. For locations within $\pm 60^{\circ}$ latitude, on average, the cost of the 2T mounting structures should be reduced by 60% to achieve the lowest LCOE among all the analyzed installations. Figure 7 also reveals that, on the one hand, the mounting structure costs for fixed-tilt and 1T systems have a small spread as these designs have already reached a high maturity level, and as such, future cost reductions are not expected to be rapid. On the other hand, the lower end costs of 2T mounting structures presented in this figure have the potential to become a viable option in the future. Further research in this topic is therefore recommended.

(5) The sensitivity analysis based on the Monte Carlo and region sensitivity approaches show that there is considerable uncertainty within the achievable LCOEs with respect to system-related parameters. While bifacial 1T systems emerge, in general, as the best performing option, local conditions can result in another system design generating lower LCOEs. Our analysis can therefore provide an overview of how systems compare on a global perspective, but to find the best performing system in any given location a detailed comparison is still necessary.

Conclusions

While literature provides research on the yield estimation for different systems, this work presented the first worldwide study on the cost-competitiveness of PV farms employing bifacial and monofacial modules with fixed-tilt mounting, single-axis and dual-axis trackers. The irradiance reaching the module front and rear sides for the different designs was estimated and validated based on the measured data from real PV systems and results from the literature. Subsequently, the PV systems' energy generation during their 25-year lifetime was estimated. The system overall cost was factored in, and the LCOE was obtained to analyze their cost effectiveness.

The results revealed that bifacial single-axis tracker installations achieved the lowest LCOE values for 93.1% of the total land area, while monofacial single-axis tracker

Table 6. Average Yield Ratio Matrix (Ratios of Column/Row) for Yield Values at Latitudes within a Range of $\pm 60^{\circ}$

	Monofacial-Fixed	Bifacial-Fixed	Monofacial-1T	Bifacial-1T	Monofacial-2T	Bifacial-2T
Monofacial-Fixed	1	1.07	1.26	1.35	1.31	1.40
Bifacial-Fixed	0.94	1	1.18	1.26	1.23	1.31
Monofacial-1T	0.79	0.85	1	1.07	1.04	1.11
Bifacial-1T	0.74	0.79	0.94	1	0.98	1.04
Monofacial-2T	0.76	0.82	0.96	1.03	1	1.07
Bifacial-2T	0.71	0.76	0.90	0.96	0.94	1

Please cite this article in press as: Rodríguez-Gallegos et al., Global Techno-Economic Performance of Bifacial and Tracking Photovoltaic Systems, Joule (2020), https://doi.org/10.1016/j.joule.2020.05.005

Table 7. Average LCOE Ratio Matrix (Ratios of Column/Row) for LCOE Values at Latitudes within a Range of ± 60°

	Monofacial-Fixed	Bifacial-Fixed	Monofacial-1T	Bifacial-1T	Monofacial-2T	Bifacial-2T
Monofacial-fixed	1	0.97	0.86	0.84	1.08	1.04
Bifacial-fixed	1.03	1	0.89	0.87	1.11	1.08
Monofacial-1T	1.16	1.12	1	0.97	1.25	1.21
Bifacial-1T	1.19	1.16	1.03	1	1.28	1.24
Monofacial-2T	0.93	0.91	0.81	0.78	1	0.97
Bifacial-2T	0.96	0.93	0.83	0.81	1.03	1

installations reached the second lowest LCOE values for 87.9% of the total land area. Although dual-axis tracker installations achieved the highest energy production, due to their current high costs, they only reached the lowest LCOE values for locations very close to the poles. This reveals that single-axis tracker installations are currently favorable in most regions of the world as they are advantageous with respect to fixed-tilt (7%–37% higher energy production within 60° latitude) and dual-axis tracker installations (8%–29% lower cost).

Sensitivity analyses based on the Monte Carlo and region sensitivity approaches were also conducted to analyze the variations on LCOE with respect to changes on the input parameters (weather, module, and cost-related parameters). These analyses show that local conditions can result in other system designs (different to bifacial single-axis tracker installations) generating the lowest LCOE.

Limitations on our approach have also been described for the reader to have a better understanding of our work, and to properly interpret our results and conclusions.

Because the land cost was neglected in this work, the module row-row distance was considered to be large enough to avoid the potential shading between neighboring rows. Nevertheless, projects with significant land cost might arise. Therefore, an approach to optimize the module row-row distance and module tilt based on the land cost influence, which has the potential to change the LCOE ranking of the various PV configurations, will be left for a future study.

This investigation can then be used as a guide to determine the suitable system technology and configuration for a particular location, which can be extremely important for PV installation companies and investors.

EXPERIMENTAL PROCEDURES

Resource Availability

Lead Contact

Further information and requests for resources and materials should be directed to and will be fulfilled by the Lead Contact, Carlos D. Rodríguez-Gallegos (carlos.rodriguez@nus.edu.sg).

Materials Availability

This study did not generate new unique materials.

Data and Code Availability

The published article includes all worldwide cost-related data generated or analyzed during this study. There are restrictions to the availability of the main code as it is property of the Solar Energy Research Institute of Singapore.

SUPPLEMENTAL INFORMATION

Supplemental Information can be found online at https://doi.org/10.1016/j.joule.2020.05.005.

ACKNOWLEDGMENTS

This work was supported by the Solar Energy Research Institute of Singapore (SERIS). SERIS is supported by the National University of Singapore (NUS) and Singapore's National Research Foundation (NRF) through the Singapore Economic Development Board (EDB). This work was also financially supported by the DOE-NSF ERF for Quantum Energy and Sustainable Solar Technologies (QESST) and by funding from Singapore's National Research Foundation through the Singapore MIT Alliance for Research and Technology's "Low energy electronic systems (LEES)" IRG. Sandia National Laboratories is a multi-mission laboratory managed and operated by National Technology & Engineering Solutions of Sandia, LLC, a wholly owned subsidiary of Honeywell International Inc., for the U.S. Department of Energy's National Nuclear Security Administration under contract DE-NA0003525. We would also like to acknowledge NASA as the source of satellite data.

AUTHOR CONTRIBUTIONS

C.D.R.-G. developed the simulations to estimate the worldwide irradiance, energy generation, costs, and LCOE of the analyzed PV systems with valuable feedback from I.M.P., H.L., O.G., J.P.S., V.K., A.K., and T.R. J.S.S. provided the data from PV systems located at the United States while L.L. and S.H. provided the validation data from PV systems located at China. Discussions with J.S.S., L.L., and S.H. also took place to properly model the performance of their PV systems. C.D.R.-G., I.M.P., H.L., and J.P.S. were involved in the initial conceptualization of the project, and I.M.P. acted as the main supervisor. The manuscript was written by C.D.R.-G. and edited by all the co-authors. All the authors reviewed and approved the manuscript.

DECLARATION OF INTERESTS

The authors declare no competing interests.

Received: January 20, 2020
Revised: March 27, 2020
Accepted: May 4, 2020
Published: June 3, 2020

REFERENCES

1. International Energy Agency (IEA) (2020). 2020 Snapshot of Global PV Markets. https://iea-pvps.org/snapshot-reports/snapshot-2020/.

2. McCrone, A. (2018). Global trends in renewable energy Investment 2018. (UN Environment's Economy Division, Frankfurt School-UNEP Collaborating Centre for Climate & Sustainable Energy Finance, and Bloomberg New Energy). https://wedocs.unep.org/bitstream/handle/20.500.11822/29752/GTR2019.pdf.

3. International Energy Agency (IEA) (2019). 2019 Snapshot of Global PV Markets. https://resources.solarbusinesshub.com/images/reports/216.pdf.

4. Pujari, N.S., Cellere, G., Falcon, T., Hage, F., Zwegers, M., Bernreuter, J., Haase, J., Yakovlev, S., Coletti, G., Romijin, I., et al. (2018). International technology roadmap for photovoltaic (ITRPV): Ninth Edition. https://pv.vdma.org/documents/105945/26776337/ITRPV%20Ninth%20Edition%202018%20including%20maturity%20report%2020180904_1536055215523.pdf/a907157c-a241-eec0-310d-fd76f1685b2a.

5. Marion, B., MacAlpine, S., Deline, C., Asgharzadeh, A., Toor, F., Riley, D., Stein, J., and Hansen, C. (2017). A practical irradiance model for bifacial PV modules. 2017 (IEEE 44th Photovoltaic Specialist Conference (PVSC)), pp. 1537–1542.

6. Pelaez, S.A., Deline, C., MacAlpine, S.M., Marion, B., Stein, J.S., and Kostuk, R.K. (2019). Comparison of bifacial solar irradiance model predictions with field validation. IEEE J. Photovoltaics 9, 82–88.

7. Bolinger, M., Seel, J., and Robson, D. (2019). Utility-Scale Solar: Empirical Trends in Project Technology, Cost, Performance, and PPA Pricing in the United States–2019 Edition. https://emp.lbl.gov/sites/default/files/lbnl_utility_scale_solar_2019_edition_final.pdf.

8. Barbose, G., Darghouth, N., LaCommare, K., Millstein, D., and Rand, J. (2018). Tracking the Sun: Installed Price Trends for Distributed Photovoltaic Systems in the United States - 2018 (Lawrence Berkeley National

Laboratory(LBNL)). https://eta-publications.lbl.gov/sites/default/files/tracking_the_sun_2018_edition_final.pdf.

9. Fu, R., Feldman, D., and Margolis, R. (2018). U.S. solar photovoltaic system cost benchmark: Q1 2018 (National Renewable Energy Laboratory, Office of Energy Efficiency and Renewable Energy). https://www.nrel.gov/docs/fy19osti/72133.pdf.

10. Janssen, G.J.M., Van Aken, B.B., Carr, A.J., and Mewe, A.A. (2015). Outdoor performance of bifacial modules by measurements and modelling. Energy Procedia *77*, 364–373.

11. Janssen, G.J.M., Burgers, A.R., Binani, A., Carr, A.J., van Aken, B.B., Romijn, I.G., Klenk, M., Nussbaumer, H., and Baumann, T. (2018). How to maximize the KWH/KWP ratio: simulations of single-axis tracking in bifacial systems. In 35th European Photovoltaic Solar Energy Conference and Exhibition (EU PVSEC). https://doi.org/10.4229/35thEUPVSEC20182018-6BO.7.5.

12. Katsaounis, T., Kotsovos, K., Gereige, I., Basaheeh, A., Abdullah, M., Khayat, A., Al-Habshi, E., Al-Saggaf, A., and Tzavaras, A.E. (2019). Performance assessment of bifacial c-Si PV modules through device simulations and outdoor measurements. Renewable Energy *143*, 1285–1298.

13. Berrian, D., Libal, J., Klenk, M., Nussbaumer, H., and Kopecek, R. (2019). Performance of bifacial PV arrays with fixed tilt and horizontal single-axis tracking: comparison of simulated and measured data. IEEE J. Photovoltaics *9*, 1583–1589.

14. Yusufoglu, U.A., Pletzer, T.M., Koduvelikulathu, L.J., Comparotto, C., Kopecek, R., and Kurz, H. (2015). Analysis of the annual performance of bifacial modules and optimization methods. IEEE J. Photovoltaics *5*, 320–328.

15. Shoukry, I., Libal, J., Kopecek, R., Wefringhaus, E., and Werner, J. (2016). Modelling of bifacial gain for stand-alone and in-field installed bifacial PV modules. Energy Procedia *92*, 600–608.

16. Vogt, M.R., Gewohn, T., Bothe, K., Schinke, C., and Brendel, R. (2018). Impact of using spectrally resolved ground albedo data for performance simulations of bifacial modules. In Proceedings of the 35th Eur. Photovolt. Sol. Energy Conference Exhibition, pp. 1011–1016.

17. Asgharzadeh, A., Lubenow, T., Sink, J., Marion, B., Deline, C., Hansen, C., Stein, J., and Toor, F. (2017). Analysis of the impact of installation parameters and system size on bifacial gain and energy yield of PV systems. In 2017 IEEE 44th Photovoltaic Specialist Conference (PVSC), pp. 3333–3338.

18. Stein, J.S., Riley, D., Lave, M., Hansen, C., Deline, C., and Toor, F. (2017). Outdoor field performance from bifacial photovoltaic modules and systems. In 2017 IEEE 44th Photovoltaic Specialist Conference (PVSC), pp. 3184–3189.

19. Stein, J.S., Burnham, L., and Lave, M. (2017). One Year Performance Results for the Prism Solar Installation at the New Mexico Regional Test Center: Field Data from February 15 2016-February 14, 2017 (Sandia National Laboratories).

20. Burnham, L., Riley, D., Walker, B., and Pearce, J.M. (2019). Performance of bifacial photovoltaic modules on a dual-axis tracker in a high-latitude, high-albedo environment. In IEEE 46th Photovoltaic Specialists Conference (PVSC), pp. 1320–1327.

21. Pelaez, S.A., Deline, C., Greenberg, P., Stein, J.S., and Kostuk, R.K. (2019). Model and validation of single-axis tracking with bifacial PV. IEEE J. Photovoltaics *9*, 715–721.

22. Asgharzadeh, A., Anoma, M.A., Hoffman1, A., Chaudhari, C., Bapat, S., Perkins, R., Cohen, D., Kimball, G.M., Riley, D., Toor, F., and Bourne, B. (2019). A benchmark and validation of bifacial PV irradiance models. In IEEE 46th Photovoltaic Specialists Conference (PVSC). 2019, pp. 3281–3287.

23. Di Stefano, A., Leotta, G., and Bizzari, F. (2017). La Silla PV plant as a utility-scale side-by-side test for innovative modules technologies. In 33rd European Photovoltaic Solar Energy Conference and Exhibition EUPVSEC, pp. 1978–1982.

24. Chudinzow, D., Haas, J., Díaz-Ferrán, G., Moreno-Leiva, S., and Eltrop, L. (2019). Simulating the energy yield of a bifacial photovoltaic power plant. Solar Energy *183*, 812–822.

25. Seo, Y., Park, H., Yoo, Y., Kim, M., Oh, S.-Y., Alhammadi, S., Chang, S., Park, S.-H., Lee, J., and Mun, S. (2019). Effect of front irradiance and albedo on bifacial gain in 1.8 kW bifacial silicon photovoltaic system. In IEEE 46th Photovoltaic Specialists Conference (PVSC). 2019, pp. 1298–1301.

26. Sugibuchi, K., Ishikawa, N., and Obara, S. (2013). Bifacial-PV power output gain in the field test using EarthON high Bifaciality solar cells. In Proceedings of the 28th European Photovoltaic Solar Energy Conference, pp. 4312–4317.

27. Guo, S., Walsh, T.M., and Peters, M. (2013). Vertically mounted bifacial photovoltaic modules: a global analysis. Energy *61*, 447–454.

28. Ito, M., and Gerritsen, E. (2016). Geographical mapping of the performance of vertically installed bifacial modules. In 32nd European Photovoltaic Solar Energy Conference and Exhibition, pp. 1603–1609.

29. Sun, X., Khan, M.R., Deline, C., and Alam, M.A. (2018). Optimization and performance of bifacial solar modules: a global perspective. Appl. Energy *212*, 1601–1610.

30. Rodríguez-Gallegos, C.D., Bieri, M., Gandhi, O., Singh, J.P., Reindl, T., and Panda, S.K. (2018). Monofacial vs bifacial Si-based PV modules: which one is more cost-effective? Sol. Energy *176*, 412–438.

31. Jacobson, M.Z., and Jadhav, V. (2018). World estimates of PV optimal tilt angles and ratios of sunlight incident upon tilted and tracked PV panels relative to horizontal panels. Sol. Energy *169*, 55–66.

32. NASA (2019). Clouds and earth's radiant energy system (CERES). https://ceres.larc.nasa.gov/.

33. Haurwitz, B. (1945). Insolation in relation to cloudiness and cloud density. J. Meteor. *2*, 154–166.

34. Haurwitz, B. (1946). Insolation in relation to cloud type. J. Meteor. *3*, 123–124.

35. Orgill, J.F., and Hollands, K.G.T. (1977). Correlation equation for hourly diffuse radiation on a horizontal surface. Sol. Energy *19*, 357–359.

36. Reda, I., and Andreas, A. (2004). Solar position algorithm for solar radiation applications. Sol. Energy *76*, 577–589.

37. Yang, D. (2016). Solar radiation on inclined surfaces: corrections and benchmarks. Sol. Energy *136*, 288–302.

38. Gueymard, C.A. (2009). Direct and indirect uncertainties in the prediction of tilted irradiance for solar engineering applications. Sol. Energy *83*, 432–444.

39. Martin, N., and Ruiz, J.M. (2001). Calculation of the PV modules angular losses under field conditions by means of an analytical model. Sol. Energy Mater. Sol. Cells *70*, 25–38.

40. Marion, B. (2017). Numerical method for angle-of-incidence correction factors for diffuse radiation incident photovoltaic modules. Sol. Energy *147*, 344–348.

41. Fanney, A.H., Davis, M.W., and Dougherty, B.P. (2002). Short-term characterization of building integrated photovoltaic panels. J. Sol. Energy Eng. *125*, 13–20.

42. Kratochvil, J.A., Boyson, W.E., and King, D.L. (2004). Photovoltaic Array Performance Model (Sandia National Laboratories). https://prod-ng.sandia.gov/techlib-noauth/access-control.cgi/2004/043535.pdf.

43. Rodríguez-Gallegos, C.D., Gandhi, O., Yang, D., Alvarez-Alvarado, M.S., Zhang, W., Reindl, T., and Panda, S.K. (2018). A siting and sizing optimization approach for PV–battery–diesel hybrid systems. IEEE Trans. Ind. Applicat. *54*, 2637–2645.

44. Rodriguez-Gallegos, C.D., Gandhi, O., Ali, J.M.Y., Shanmugam, V., Reindl, T., and Panda, S.K. (2019). On the grid metallization optimization design for monofacial and bifacial Si-based PV modules for real-world conditions. IEEE J. Photovoltaics *9*, 112–118.

45. Yang, D., Liu, L., Rodríguez-Gallegos, C.D., Ye, Z., and Lim, L.H.I. (2017). Statistical modeling, parameter estimation and measurement planning for PV degradation. In Solar Energy and Solar Panels: Systems, Performance and Recent Developments, J.G. Carter, ed. (Nova Science Publishers, Inc.)), pp. 1–22.

46. Rodríguez-Gallegos, C.D., Gandhi, O., Bieri, M., Reindl, T., and Panda, S.K. (2018). A diesel replacement strategy for off-grid systems based on progressive introduction of PV and batteries: an Indonesian case study. Appl. Energy *229*, 1218–1232.

47. Rodríguez-Gallegos, C.D., Yang, D., Gandhi, O., Bieri, M., Reindl, T., and Panda, S.K. (2018). A multi-objective and robust optimization approach for sizing and placement of PV & batteries in off-grid systems fully operated by diesel generators: an Indonesian case study. Energy *160*, 410–429.

48. Bieri, M., Winter, K., Tay, S., Chua, A., and Reindl, T. (2017). An irradiance-neutral view on the competitiveness of life-cycle cost of PV

rooftop systems across cities. Energy Procedia *130*, 122–129.

49. NexTracker. (2019). NX Horizon: self-powered tracker. https://www.nextracker.com/wp-content/uploads/2017/12/NXHorizon120.Brochure_April2017.pdf.

50. Soltec. (2019). SF7: one track zero gap. https://soltec.com/wp-content/uploads/2018/05/Datasheet-SF7-US-2018.pdf.

51. GameChange Solar. (2019). Genius Tracker: world's highest power producing and fastest installing solar tracker. https://gamechangesolar.com/downloads/Technical_Datasheet_Genius_Tracker.pdf.

52. Axsus. (2019). Sol-X tracker. https://www.axsussolar.com/wp-content/uploads/2019/06/Axsus_Datasheet_Sol-X_v4.pdf.

53. Arctech Solar. (2019). Skyline tracking system. http://www.arctechsolar.us/index.php/product/skyline_tracking.

54. Nclave. (2019). Self-Powered solar tracker SP160. http://www.nclavegroup.com/en/product/self-powered-solar-tracker-sp160.

55. Mitbet. (2019). MRac smart horizontal single axis tracking solar PV mounting system. https://www.mbt-energy.com/Content/Upload/2018-11-15/201811151120543237.pdf.

56. Marion, W.F., and Dobos, A.P. (2013). Rotation Angle for the Optimum Tracking of One-Axis Trackers (National Renewable Energy Laboratory, Office of Energy Efficiency and Renewable Energy). https://www.nrel.gov/docs/fy13osti/58891.pdf.

57. Bieri, M., Kumar, A., Aberle, A., and Reindl, T. (2016). Economic viability analysis of solar cell manufacturing. 26th International Photovoltaic Science and Engineering Conference (PVSEC-26), 1–4.

58. Kumar, A., Bieri, M., Reindl, T., and Aberle, A.G. (2017). Economic Viability Analysis of Silicon Solar Cell Manufacturing: Al, BSF versus PERC. Energy Procedia *130*, 43–49.

59. Kumar, A. (2018). Economic competitiveness of high-efficiency mono-Si solar cells: $/Wp manufacturing cost & end-user LCOE (Renewable Energy India Expo), pp. 1–15.

60. LONGiSolar. (2019). LR6-60PE: 300–320M. http://polaronsolar.com/wp-content/uploads/2018/12/LR6-60PE-300-320M_polaron-logo.pdf.

61. LONGiSolar. (2019). LR6-60BP: 295–315M. https://solar-distribution.baywa-re.lu/fileadmin/Solar_Distribution_Benelux/04_Products/03_Media/LONGi/Datenblaetter/20180901_LONGi_Data_Sheet_LR6-60BP_295-315M_LowRes_EN.pdf.

62. Trading economics. (2019). Markets: bonds. https://tradingeconomics.com/bonds.

63. International Monetary Fund (2019). Inflation rate, average consumer prices. http://www.imf.org/external/datamapper/PCPIPCH@WEO/OEMDC/ADVEC/WEOWORLD.

64. Fernandez, P., Ortiz, P.A., and Acín, I.F. (2016). Market risk premium used in 71 countries in 2016: a survey with 6,932 answers (SSRN). https://doi.org/10.2139/ssrn.2776636.

65. Damodaran, A. (2019). Country default spreads and risk premiums. http://pages.stern.nyu.edu/~adamodar/New_Home_Page/datafile/ctryprem.html.

66. Trading Economics. (2019). List of countries by corporate tax rate. https://tradingeconomics.com/country-list/corporate-tax-rate.

67. Wikipedia (2019). List of minimum wages by country (Wikipedia). https://en.wikipedia.org/wiki/List_of_minimum_wages_by_country#cite_note-CRHRP-2012-8.

68. Mega Engineering. (2015). Installation rules to maximize bifacial solar modules performances.

69. Chang, N.L., Ho-Baillie, A.W.Y., Vak, D., Gao, M., Green, M.A., and Egan, R.J. (2018). Manufacturing cost and market potential analysis of demonstrated roll-to-roll perovskite photovoltaic cell processes. Sol. Energy Mater. Sol. Cells *174*, 314–324.

70. Green rhino energy (2019). Annual solar irradiance, intermittency and annual variations. 2019. http://www.greenrhinoenergy.com/solar/radiation/empiricalevidence.php.

71. PVinsights. (2019). Solar PV Module Weekly Spot Price. http://pvinsights.com/.